# The CDC50A extracellular domain is required for forming a functional complex with and chaperoning phospholipid flippases to the plasma membrane

Received for publication, October 5, 2017, and in revised form, December 21, 2017 Published, Papers in Press, December 24, 2017, DOI 10.1074/jbc.RA117.000289

**Katsumori Segawa, Sachiko Kurata, and Shigekazu Nagata**[1]

*From the Laboratory of Biochemistry and Immunology, Immunology Frontier Research Center, Osaka University, Suita, Osaka 565-0871, Japan*

Edited by George M. Carman

**Flippases are enzymes that translocate phosphatidylserine (PtdSer) and phosphatidylethanolamine (PtdEtn) from the outer to the inner leaflet in the lipid bilayer of the plasma membrane, leading to the asymmetric distribution of aminophospholipids in the membrane. One mammalian phospholipid flippase at the plasma membrane is ATP11C, a type IV P-type ATPase (P4-ATPase) that forms a heterocomplex with the transmembrane protein CDC50A. However, the structural features in CDC50A that support the function of ATP11C and other P4-ATPases have not been characterized. Here, using error-prone PCR-mediated mutagenesis of human *CDC50A* cDNA followed by functional screening and deep sequencing, we identified 14 amino acid residues that affect ATP11C's flippase activity. These residues were all located in CDC50A's extracellular domain and were evolutionarily well-conserved. Most of the mutations decreased CDC50A's ability to chaperone ATP11C and other P4-ATPases to their destinations. The CDC50A mutants failed to form a stable complex with ATP11C and could not induce ATP11C's PtdSer-dependent ATPase activity. Notably, one mutant variant could form a stable complex with ATP11C and transfer ATP11C to the plasma membrane, yet the ATP11C complexed with this CDC50A variant had very weak or little PtdSer- or PtdEtn-dependent ATPase activity. These results indicated that the extracellular domain of CDC50A has important roles both in CDC50A's ability to chaperone ATP11C to the plasma membrane and in inducing ATP11C's ATP hydrolysis-coupled flippase activity.**

In the plasma membranes of eukaryotes, phospholipids are asymmetrically distributed between the lipid bilayers; aminophospholipids such as phosphatidylserine (PtdSer)[2] and phosphatidylethanolamine (PtdEtn) are confined to the inner leaflet, whereas phosphatidylcholine and sphingomyelin are enriched in the outer one (1, 2). In various biological processes, this non-random distribution of phospholipids is disrupted, exposing PtdSer on the cell surface as a signal for surrounding cells or proteins (3). Apoptotic cell clearance and blood clotting are well-established PtdSer-mediated processes; the PtdSer on apoptotic cells functions as an "eat me" signal to be recognized by phagocytes for engulfment (4, 5), whereas the PtdSer on activated platelets acts as a scaffold for blood-clotting factors (6).

Phospholipids rarely flip spontaneously across the hydrophobic lipid bilayers of membranes, due to their amphipathic nature (7). Instead, transverse phospholipid movements are facilitated by three types of enzymes in the membrane, called flippases, floppases, and scramblases (1, 2). Coupled with ATP hydrolysis, flippases specifically translocate PtdSer and PtdEtn from the outer to inner leaflet of the cell membrane, establishing the asymmetrical distribution of PtdSer and PtdEtn between the two leaflets (8), whereas scramblases bidirectionally and nonspecifically translocate phospholipids across the lipid bilayers without consuming ATP.

In eukaryotes, type IV P-type ATPases (P4-ATPases), which carry 10 transmembrane segments, have been proposed to be flippases (8, 9). The human and mouse genomes encode 14 and 15 P4-ATPase members, respectively. Different P4-ATPase members are localized to the plasma membrane, endoplasmic reticulum (ER), lysosomes, Golgi apparatus, or recycling endosomes (10). We previously showed that ATP11A and ATP11C are localized to the plasma membrane in human and mouse lymphocytes and function as flippases (11, 12). Recent reports using *ATP11C*-deficient mice and human patients showed that ATP11C is critical for maintaining the PtdSer asymmetry of the plasma membrane in some blood cell types (13–15).

P4-ATPases except for ATP9A and ATP9B form a heterodimer with CDC50A, and CDC50A has been proposed to be

This work was supported in part by Grants-in-Aid for Scientific Research on Innovative Areas 16H01360 and 17H05506 from the Japan Society for the Promotion of Science (to K. S.), Grant-in-Aid for Specially Promoted Research 15H05785 from the Japan Society for the Promotion of Science (to S. N.), and Grant-in-Aid JPMJCR14M4 from Core Research for Evolutional Science and Technology, Japan Science and Technology Agency (to S. N.). The authors declare that they have no conflicts of interest with the contents of this article.

This article contains Tables S1–S3 and Figs. S1–S3.

[1] To whom correspondence should be addressed. Tel.: 81-6-6879-4953; Fax: 81-6-6879-4950; E-mail: snagata@ifrec.osaka-u.ac.jp.

[2] The abbreviations used are: PtdSer, phosphatidylserine; ER, endoplasmic reticulum; P4-ATPase, type IV P-type ATPase; PtdEtn, phosphatidylethanolamine; NBD-PS, 1-oleoyl-2-{6-[(7-nitro-2–1,3-benzoxadiazol-4-yl)amino]hexanoyl}-*sn*-glycero-3-phosphoserine; NBD-PE, 1-oleoyl-2-{6-[(7-nitro-2–1,3-benzoxadiazol-4-yl)amino]hexanoyl}-*sn*-glycero-3-phosphoethanolamine; POPS, 1-palmitoyl-2-oleoyl-*sn*-glycero-3-phospho-L-serine; POPE, 1-palmitoyl-2-oleoyl-*sn*-glycero-3-phosphoethanolamine; HBSS, Hank's balanced salt solution; CBB, Coomassie Brilliant Blue; LMNG, lauryl maltose-neopentyl glycol; LF, lost-flippase; Ab, antibody, mAb, monoclonal antibody; HRP, horseradish peroxidase; MFI, median fluorescence intensity.

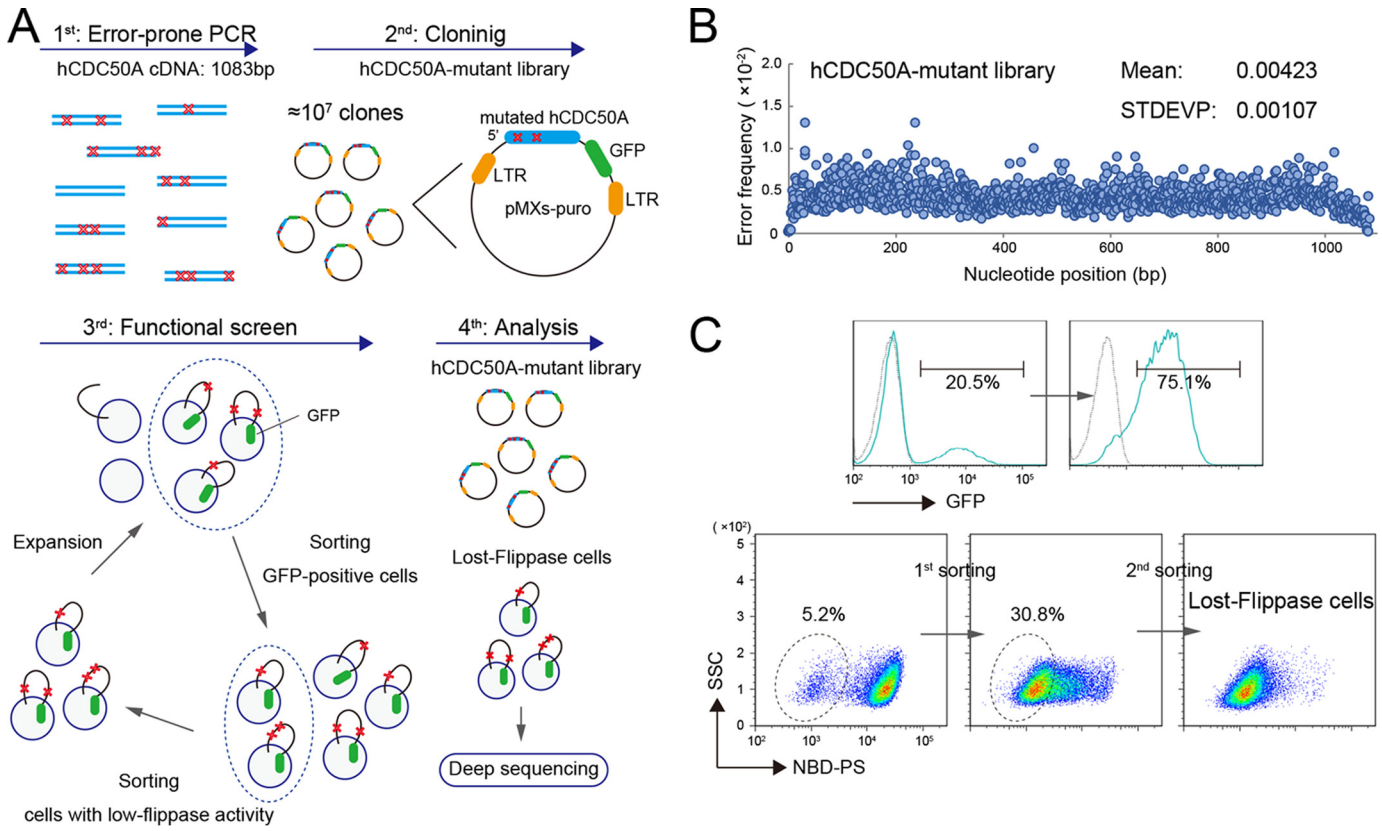


**Figure 1. Identification of loss-of-function mutations in human CDC50A.** *A*, construction of mutant library and screening. In the first step, mutations were randomly introduced into the *hCDC50A* cDNA by error-prone PCR. In the second step, the PCR products were incorporated into pMXs-puro-GFP to generate a hCDC50A mutant library. In the third step, CDC50A$^{ED29}$ cells were transformed with the mutant library and subjected to repetitive cell sorting to enrich for GFP-positive cells with low PtdSer flippase activity (lost-flippase cells). In the fourth step, the mutations were identified by deep sequencing, and the read sequences were processed to determine the mutation frequency. *B*, error frequency in the hCDC50A mutant library. The error frequency at each nucleotide position in the mutant library was calculated and plotted. Mean and S.D. values are shown. *C*, isolation of cells with low flippase activity by cell sorting. In the *top left panel*, CDC50A$^{ED29}$ cells transformed by the CDC50A mutant library (*blue*) were sorted for GFP. The *top right panel* shows the GFP-sorted transformants (*blue*). The GFP profile of the parental CDC50A$^{ED29}$ cells is in *gray*. The percentage of GFP-positive cells is indicated. In the *bottom panels*, the flippase activity in the sorted GFP-positive cells was assayed by the incorporation of NBD-PS. The cells that failed to incorporate NBD-PS were enriched by two rounds of cell sorting and designated as lost-flippase cells. The percentage of sorted cells in each round is shown.

a $\beta$-subunit of the flippase complex (8). CDC50A belongs to the CDC50 family of membrane proteins, which carry two transmembrane segments with short N- and C-cytoplasmic regions and a large extracellular loop (8). There are three CDC50 family members in humans and mice: CDC50A, CDC50B, and CDC50C (also referred to as TMEM30A, TMEM30B, and TMEM30C). CDC50 proteins appear to be critical for the proper folding of P4-ATPases and for chaperoning them to their final subcellular locations (10, 16). Accordingly, P4-type ATPases that require CDC50A as a partner fail to exit the ER in the absence of CDC50A (11).

In this report, we generated human CDC50A (hCDC50A) cDNA mutants by error-prone PCR and expressed them in *CDC50A*-null T-lymphoma cells. The flippase activity at plasma membranes was assayed by the incorporation of a fluorescently labeled PtdSer analogue, and the cells exhibiting low flippase activity were enriched by repetitive cell sorting. The cells in this population, designated as lost-flippase (LF) cells, were subjected to deep sequencing analysis, which identified 14 amino acid residues that were important for CDC50A's ability to support ATP11C's flippase activity. These residues were located in CDC50A's extracellular loop and were evolutionarily well-conserved in eukaryotes. Most of the mutations impaired CDC50A's chaperoning activity. In contrast, one mutation of CDC50A had little effect on its complex formation with ATP11C, and ATP11C with this mutant CDC50A was found at the plasma membrane. However, its phospholipid-dependent ATPase activity was dramatically decreased, indicating that, in addition to its chaperone function, CDC50A plays a direct role in ATP11C's flippase activity.

## Results

### *Mutagenesis and enrichment of cells expressing non-functional CDC50A*

To investigate CDC50A's functions, mutations were randomly introduced into the *hCDC50A* cDNA sequence (1083 bp) by error-prone PCR using low-fidelity DNA polymerase. The mutated cDNA was fused to GFP at the C terminus, introduced into pMXs-puro, and used to transform *Escherichia coli* to obtain about $1 \times 10^7$ clones for the mutant library (Fig. 1*A*). Deep sequencing analysis of the hCDC50A mutant library indicated that the mutations were uniformly introduced throughout the *hCDC50A* cDNA at an average error rate of 0.00423, ~4 mutations per cDNA (Fig. 1*B*). This result was confirmed by the sequencing of several clones.

We previously reported that a mouse lymphoma cell line, CDC50A$^{ED29}$, which is a *CDC50A*-null WR19L line, lacks plasma membrane flippase activity for PtdSer (12). We therefore used this cell line to identify loss-of-function mutations in hCDC50A. Retroviruses carrying each GFP-tagged CDC50A mutant were produced in HEK293T cells by transfecting them with the pMX-puro–based hCDC50A mutant library. The retroviruses were then used to infect $3.8 \times 10^7$ CDC50A$^{ED29}$ cells at a low multiplicity of infection to achieve less than one viral insertion per host cell. Flow cytometry analysis of the infected cells showed that about 20% of the cells expressed GFP (Fig. 1*C*). The GFP-positive population was collected by sorting, which should remove the transformants expressing hCDC50A with nonsense and/or frameshift mutations. The GFP-positive transformants were then incubated with 1 $\mu$M 1-Oleoyl-2-{6-[(7-nitro-2–1,3-benzoxadiazol-4-yl) amino]hexanoyl}-*sn*-glycero-3-phosphoserine (NBD-PS) for 5 min, and the cell population that failed to incorporate NBD-PS (about 5%) was isolated by sorting (Fig. 1*C*). This procedure, the incubation with NBD-PS, followed by sorting for GFP-positive and NBD-PS–negative, was repeated, and the resultant cells were designated as LF cells.

### *Deep sequencing*

To analyze the *hCDC50A* cDNA mutations in the LF cells, the hCDC50A sequence was amplified by PCR from LF cells and was analyzed by deep sequencing. As shown in Fig. S1, the error rate in the hCDC50A sequence increased in LF cells at several nucleotide positions. By calculating the error rates of the three nucleotides for each codon, the error frequency at each amino acid was determined (Table S1). The average frequency of mutation in the hCDC50A protein (361 amino acids) was 0.0042 in the original library, but it increased to 0.0067 in LF cells (Fig. 2*A*). The error rate of the amino acid residues of hCDC50A in LF cells divided by that of the hCDC50A mutant library was defined as the "-fold enrichment." In Fig. 2*B*, the -fold enrichment in the error rate was plotted for each amino acid residue. The highest value (5.95) was obtained at Cys-104, and 19 residues showed a -fold enrichment of >3.1 (putative outliers, the mean plus 2 times its S.D.), which was regarded as significant. For these 19 residues, the -fold enrichment in the error rate was calculated for each nucleotide, and these data are shown in Table S2 together with the replaced amino acid. This analysis showed that the -fold enrichment to conservative amino acid substitutions was not high, and non-sense mutations were not enriched. The Leu-266 residue was ranked 18th in -fold enrichment, because the third codon (A) for Leu-266 was frequently mutated to G in LF cells (Table S1). However, because this mutation did not alter the amino acid, this mutant was omitted from the functional study of the CDC50A protein. This mutation may affect the mRNA stability or the translational activity of CDC50A.

### *CDC50A mutations that impair PtdSer flippase activity*

The error-prone PCR-mediated mutagenesis should produce the replacement of an amino acid by a maximum of 9 different residues if we assume a single mutation in one codon. In fact, the 18 amino acid residues described above were each

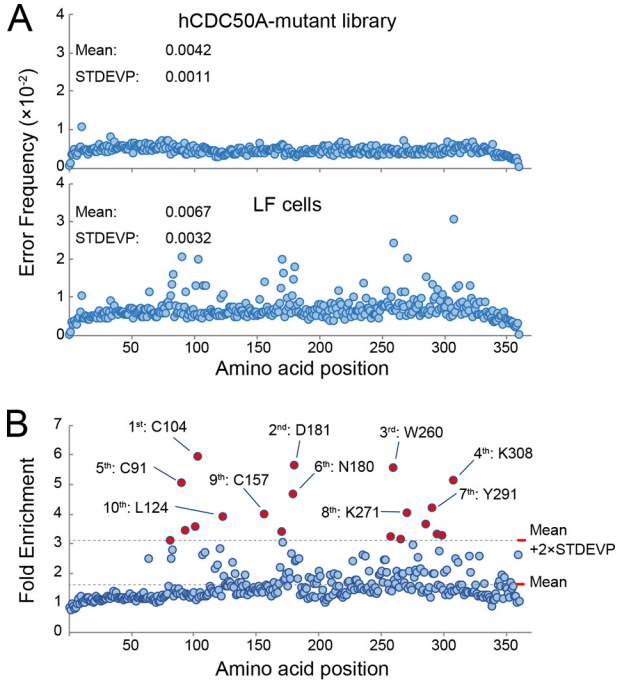


**Figure 2. Loss-of-function mutations in hCDC50A.** *A*, error rates at the indicated amino acid positions of the original hCDC50A mutant library (*top*), and of the *hCDC50A* cDNA in LF cells (*bottom*). Mean error rates and S.D. values are shown. *B*, enrichment of the error frequency in LF cells. The error rate of the respective amino acid residues of hCDC50A in LF cells was divided by that of the hCDC50A mutant library and was plotted as the -fold enrichment. The mean value (1.598) and mean plus 2 × S.D. (3.098) are indicated by *dotted lines*. The 19 residues with the highest -fold enrichment (>3.098) are *colored* in *red*, and the top 10 amino acids (Cys-91, Cys-104, Leu-124, Cys-157, Asn-180, Asp-181, Trp-260, Lys-271, Tyr-291, and Lys-308) are indicated.

mutated to 4–7 different amino acids, and the -fold enrichment in the mutation rate differed among the amino acid residues replacing a specific residue (Table S2), indicating that not only the mutation of a certain residue *per se* but also the replacing residue contributed to the loss of flippase activity.

To verify the contribution of the 18 amino acid residues to the function of CDC50A, the amino acid at each residue was changed to the amino acid that was frequently found in LF cells (*i.e.* Y82N, C91S, C94R, C102Y, C104S, L124P, C157Y, C171R, N180D, D181G, I258V, W260R, K271E, L286S, Y291N, V295D, Y299N, and K308E) (Table S2). These constructs were then FLAG-tagged at the C terminus and stably expressed in CDC50A$^{ED4}$ cells together with GFP-tagged hATP11C (Fig. 3). Western blotting analysis with anti-GFP and anti-FLAG antibodies indicated that the GFP-tagged hATP11C and FLAG-tagged hCDC50A were expressed in similar amounts among the transformants (Fig. 3*A*). The N180D mutant migrated faster (<50 kDa) than the others on SDS-PAGE, probably due to the loss of an *N*-glycosylation site (17).

We then examined the PtdSer flippase activity of the transformants expressing hATP11C with or without wildtype or mutant hCDC50A and found that the 18 CDC50A mutants could be categorized into three groups (Fig. 3*B*). The first group contained 10 mutants (Y82N, C94R, C104S, L124P, D181G, W260R, K271E, Y291N, V295D, and K308E) that supported the ATP11C's flippase activity with an efficiency less than 20% of that of wildtype CDC50A. In particular, three mutants, D181G,

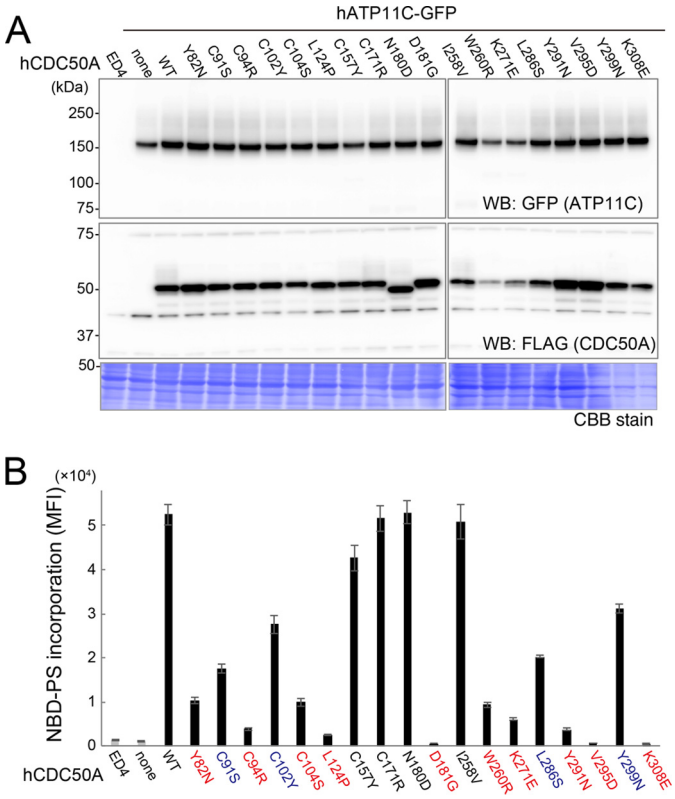


**Figure 3. Effect of CDC50A mutations on the ATP11C-mediated flippase activity**. *A*, expression of hATP11C and the hCDC50A mutants in *CDC50A*-null cells. $CDC50A^{ED4}$ cells were transformed with GFP-tagged hATP11C alone or together with FLAG-tagged WT or the indicated mutant hCDC50A. The cell lysates (10 $\mu$g of protein) were separated by SDS-PAGE and analyzed by Western blotting with an HRP-conjugated rabbit anti-GFP Ab (*top*) or mouse anti-FLAG mAb (*middle*). *Bottom*, the membrane was stained by CBB. *B*, incorporation of NBD-PS. The flippase activity of the $CDC50A^{ED4}$ transformants expressing ATP11C with or without the wildtype or indicated mutants of hCDC50A was determined by the incorporation of NBD-PS using flow cytometry. The experiments were carried out three times, and the mean median fluorescence intensity (MFI) was plotted with S.D. (*error bars*). The CDC50A mutants were divided into three groups. In groups 1, 2, and 3, indicated by *red*, *blue*, and *black*, respectively, the ability to support ATP11C's PtdSer flippase activity was reduced to 0–20, 20–60, and >60% of the wildtype CDC50A, respectively. *WB*, Western blotting.

V295D, and K308E, almost completely lost the ability to support flippase activity. The second group of mutants, C91S, C102Y, L286S, and Y299N, had a partial defect; the transformants expressing these mutants had 20–60% of the flippase activity of wildtype CDC50A. The third group of mutants (C157Y, C171R, N180D, and I258V) could support the flippase activity with an efficiency comparable with that of wildtype CDC50A, suggesting that these mutations had a defect only in combination with other mutations or that they were bystander mutations or artificially enriched during cell sorting. Overall, 14 of the 18 mutants significantly affected the function of CDC50A. These 14 amino acid residues were scattered throughout the extracellular loop region of CDC50A and are highly conserved in eukaryotes (Fig. 4).

### *Effect of CDC50A's mutations on the localization of P4-ATPases*

We next examined the localization of hATP11C. As found previously (12), GFP-hATP11C was localized intracellularly in the absence of CDC50A (Fig. 5*A*). However, this localization was changed to the plasma membrane in the presence of wildtype hCDC50A. Except for those transformed with W260R and Y299N, the cells expressing CDC50A mutants showed an intracellular localization of GFP-hATP11C (Fig. 5*A*), suggesting that the low flippase activity of these transformants (Fig. 3*B*) was due to an inefficient chaperone activity of the CDC50A mutants. In the Y299N transformants, the GFP-hATP11C was partially localized to the plasma membrane (Fig. 5*A*), which may explain the relatively high (>50% of wildtype) PtdSer flippase activity of these transformants. On the other hand, the GFP-hATP11C in W260R transformants was localized to the plasma membrane to a similar extent as the Y299N transformants, yet their flippase activity was much lower than that of the Tyr-299 transformant (about 20% of wildtype). These results suggested that the W260R mutation affects a non-chaperone-related aspect of ATP11C's flippase activity.

CDC50A chaperones not only ATP11C but also other P4-ATPases (11). To examine whether the identified mutations also affected CDC50A's chaperoning activity for ATP11A to the plasma membrane and for ATP10B to lysosomes, $CDC50A^{ED4}$ cells were co-transformed with CDC50A and GFP-tagged ATP11A or ATP10B. As reported previously (11), the GFP signal of ATP10B was intracellularly observed in the presence of the wildtype CDC50A and was co-localized with Lysotracker, a lysosome membrane marker (Fig. S2). As found with ATP11C, four mutations (C94R, D181G, V295D, and K308E) impaired CDC50A's ability to chaperone ATP10B, and the GFP signals were broadly spread around the nucleus, probably at the ER (Fig. 5*B*), whereas, in the presence of the W260R mutant, ATP10B was partially localized at lysosomes. Similarly, the wildtype CDC50A as well as W260R mutant caused ATP11A to localize to the plasma membrane, whereas the other four mutants did not (Fig. 5*C*). These results indicated that the above identified amino acid residues of CDC50A (C94R, D181G, V295D, and K308E) are critical for its ability to chaperone various P4-ATPases from the ER to their proper destinations, whereas the W260R mutant has a defect in an activity other than CDC50A's chaperoning activity.

### *Effect of the CDC50A mutations on the ATPase activity of the flippase*

The ATP11C has the flippase activity not only for PtdSer, but also for PtdEtn (12). The W260R mutation affected the ATP11C's flippase activity for PtdEtn (Fig. 6*A*) and the ATP11A's flippase activity for PtdSer (Fig. 6*B*). To examine whether the loss of the tryptophan residue at 260 affected the flippase activity or the replaced arginine inactivated the flippase activity, the tryptophan residue was replaced to alanine or lysine. As shown in Fig. 6*C*, both W260A and W260K mutants chaperoned ATP11C-GFP to the plasma membranes. On the other hand, the ability to support the ATP11C's flippase activity was reduced with both mutants, as found with the W260R mutant (Fig. 6*C*). The reduction of the flippase activity with the W260A mutant was relatively milder than that observed with the W260R and W260K mutants. These results indicated that the evolutionarily well-conserved tryptophan residue at position 260 plays an important role in CDC50A's function, and its change to a basic amino acid further destroys its function.

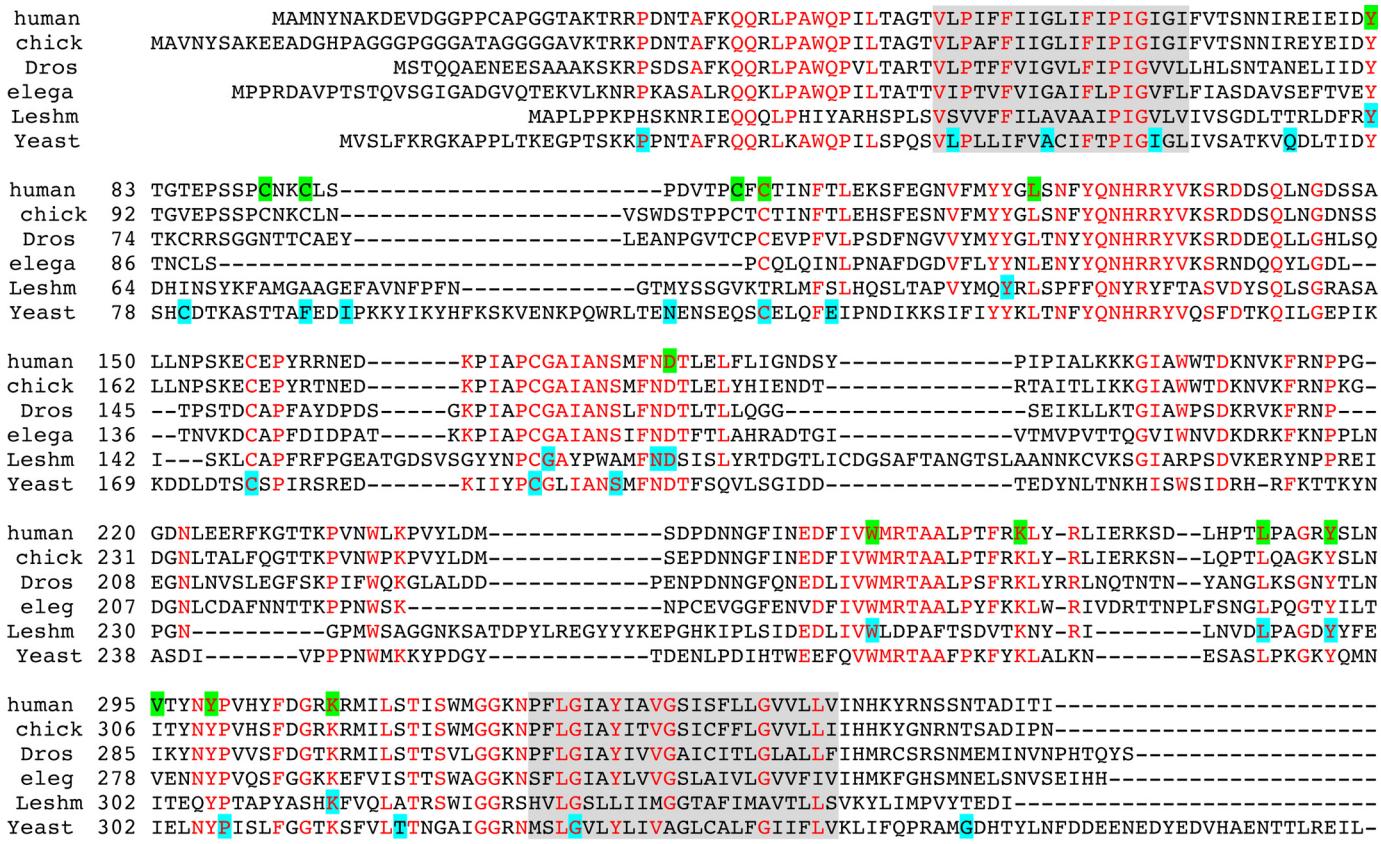


**Figure 4. Alignment of the amino acid sequences of CDC50 proteins.** Using the MAFFT program (45), the amino acid sequences of human CDC50A (NP_060717.1), chicken CDC50A (NP_001012897.1), *Drosophila* CG9947 (NP_573128.2), *C. elegans* CHAT-1 (NP_001023332.1), *Leishmania* miltefosine transporter $\beta$ subunit (ABB05176.1), and yeast CDC50p (AJQ32580.1) were aligned to obtain maximum homology. The amino acid residues that were conserved among at least five members are in *red*. The residues whose mutation reduced the ATP11C-mediated flippase activity are highlighted in *green*. The residues with identified functions in *Leishmania* (24) and yeast CDC50 (22, 23) are highlighted in *blue*.

To investigate on which aspect of the flippase activity the W260R mutant had an effect, the structure and ATPase activity of the flippase complex were then examined. The hCDC50A of the wildtype, W260R, and three mutants (D181G, V295D, and K308E) that elicited no flippase activity was GFP-tagged at the C terminus and expressed together with FLAG-tagged hATP11C in HEK293T cells, and the CDC50A-ATP11C complex was affinity-purified with an anti-FLAG mAb. Analysis of the purified complex by SDS-PAGE followed by Coomassie Brilliant Blue (CBB) staining indicated that hATP11C of the expected size (about 120 kDa) was equally recovered (Fig. 7*A*). The hCDC50A protein was recovered as broad bands of about 65–75 kDa, which was confirmed by Western blotting with an anti-GFP antibody (Ab) (Fig. 7*B*). The hCDC50A protein consists of 361 amino acids with a calculated $M_r$ of 40,682 and carries four *N*-glycosylation sites (amino acid positions 107, 180, 190, and 294), suggesting that the 65 kDa band was non-glycosylated CDC50A fused to GFP, whereas the broad bands at 75 kDa were its glycosylated forms. Except for the cells expressing the W260R mutant, which had at least partial ATP11C-chaperoning activity, the 75-kDa glycosylated form of CDC50A was not recovered as a complex with ATP11C from the cells expressing the mutant CDC50A. These results suggested that the flippase complex formed with the D181G, V295D, or K308E mutant CDC50A could not exit the ER for the Golgi apparatus, where most of the *N*-linked oligosaccharides are further modified with complex sugars (18). The purified flippase complexes were then analyzed by Blue native (BN)-PAGE (Fig. 7*C*). Western blotting with anti-FLAG for ATP11C and anti-GFP for CDC50A indicated that most of the ATP11C purified from the transformants expressing wildtype CDC50A existed as a 480-kDa complex. Because membrane proteins have a $M_r$ on native gels 1.8 times higher than the expected $M_r$ (19), the 480-kDa complex was probably a 1:1 complex of FLAG-ATP11C (calculated $M_r$ of 135,000) with CDC50A-GFP (75,000; $M_r$ calculated from its amino acid composition and sugar moieties). A flippase complex with a similar size, recognized by both anti-FLAG and anti-GFP, was observed for the ATP11C-W260R CDC50A complex, whereas most of the flippase complexes with other mutant CDC50As were found at a higher $M_r$, probably in aggregated forms (Fig. 7*C*). These results indicated that the W260R mutant but not the D181G, V295D, or K308E mutant forms a stable complex with ATP11C as efficiently as the wildtype CDC50A.

We then examined the PtdSer-activated ATPase activity of the flippase complex formed with the wildtype or the four mutant CDC50As. As shown in Fig. 7*D*, little ATPase activity was detected with ATP11C associated with the CDC50A mutants D181G, V295D, or K308E, indicating that ATP11C required the properly associated CDC50A for its ATPase activity. Notably, the PtdSer- or PtdEtn-activated ATPase activity of the ATP11C flippase complex formed with the W260R mutant

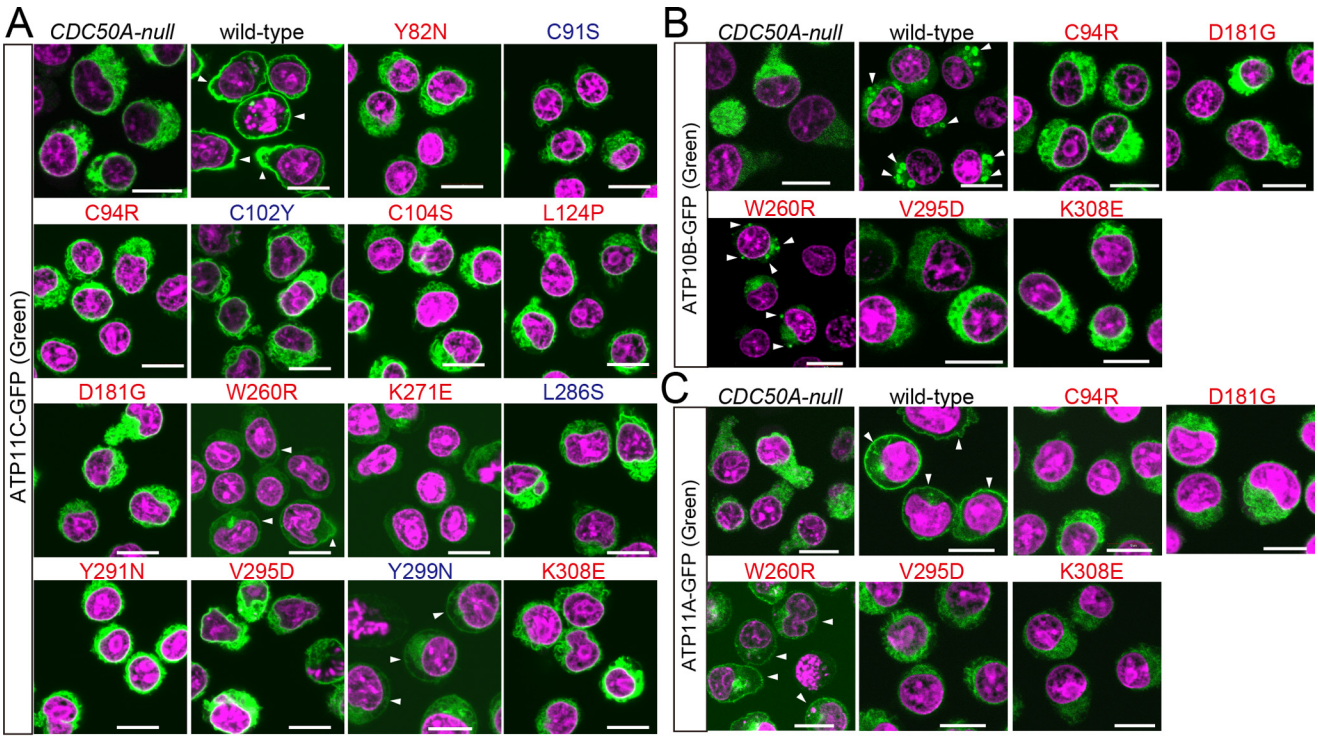


**Figure 5. Chaperone activity of CDC50A mutants for P4-ATPases.** *A–C*, effect of CDC50A mutations on the cellular localization of hATP11C (*A*), hATP10B (*B*), and hATP11A (*C*). CDC50A$^{ED4}$ cells were co-transformed with GFP-conjugated hATP11C (*A*), hATP10B (*B*), or hATP11A (*C*), together with FLAG-tagged WT or the indicated mutant CDC50A, and observed by confocal microscopy in the presence of 5 $\mu$M DRAQ5. GFP (ATP11C, ATP10B, or ATP11A) and DRAQ5 (nucleus) signals are shown in *green* and *magenta*, respectively. *Scale bar*, 10 $\mu$m. The CDC50A mutants belonging to groups 1 and 2 are indicated in *red* and *blue*, respectively. *Arrowheads*, ATP11C (*A*) and ATP11A (*C*) at plasma membranes or ATP10B at lysosomes (*B*).

was 14–28% of that with the wildtype CDC50A (Fig. 7, *D* and *E*). On the other hand, the half-maximum activation constants ($K_a$) for PtdSer were similar between the complexes with the wildtype or W260R mutant (WT = 0.8 $\mu$M, W260R = 1.4 $\mu$M). These results suggest that the W260R mutation affects ATP11C's catalytic reaction with little effect on the affinity of the ATP11C-CDC50A complex to PtdSer.

## Discussion

CDC50 is an evolutionarily well-conserved protein in eukaryotes, and its chaperone activity for P4-ATPases is well-established, but its detailed function has been elusive (8, 12, 20). CDC50 is associated with P4-ATPases at their destination sites, such as the plasma membrane and lysosome membranes, and it has been proposed to contribute to the ATPase activity, but no clear mechanism has been shown (21). To address these questions, detailed structure-function information about P4-ATPase and CDC50 is needed. The yeast CDC50 was mutagenized by a PCR-based procedure (22) or hydroxylamine (23), and several mutants were shown to have a defect in the functional complex formation with P4-ATPase. Recently, the highly evolutionarily conserved residues of the *Leishmania* CDC50 were mutated by an alanine-scanning procedure (24), and residues in the extracellular region were shown to be important for transporting the ATPase to the plasma membrane. Surprisingly, most of the residues identified in *Leishmania* differed from those identified in yeast CDC50 (24).

Among the three CDC50 genes present in humans and mice, mouse WR19L cells express only CDC50A, and CDC50A-deficient WR19L cells lose their flippase activity (12). Using this cell line as a host, we here identified the functional residues of hCDC50A by high-throughout random mutagenesis followed by deep sequencing (25, 26). We introduced mutations by error-prone PCR, because this procedure can cause the replacement of an amino acid with different residues (27), one of which may have a strong effect. In addition, this procedure was recently improved technically to generate unbiased mutations (28). In fact, the mutations were found equally at purine and pyrimidine residues in the *hCDC50A* cDNA mutant library, and the ratio of transitions to transversions was nearly 1.0. The CDC50A non-functional mutations were then selected by introducing the library into *CDC50A*-null cells, isolating the transformants with low flippase activity, and performing high-throughout sequencing of the *CDC50A* cDNA of the transformants.

All 14 of the hCDC50A mutations identified in this study were located at its extracellular region. Except for 4 cysteine residues at the N terminus, all of the other residues were well-conserved in eukaryotes, with the same or conservative amino acids found in chicken, *Drosophila*, *Caenorhabditis elegans*, *Leishmania*, and yeast CDC50 (Fig. 4). Among the 9 residues identified as being functionally important in *Leishmania* CDC50 by Ala scanning (24), 6 residues were also identified here as important residues in hCDC50A (Fig. 4). On the other hand, the 15 residues identified in yeast CDC50 (22, 23) were not critical for the hCDC50A function except for one cysteine at position 104, which seems to be involved in disulfide bond

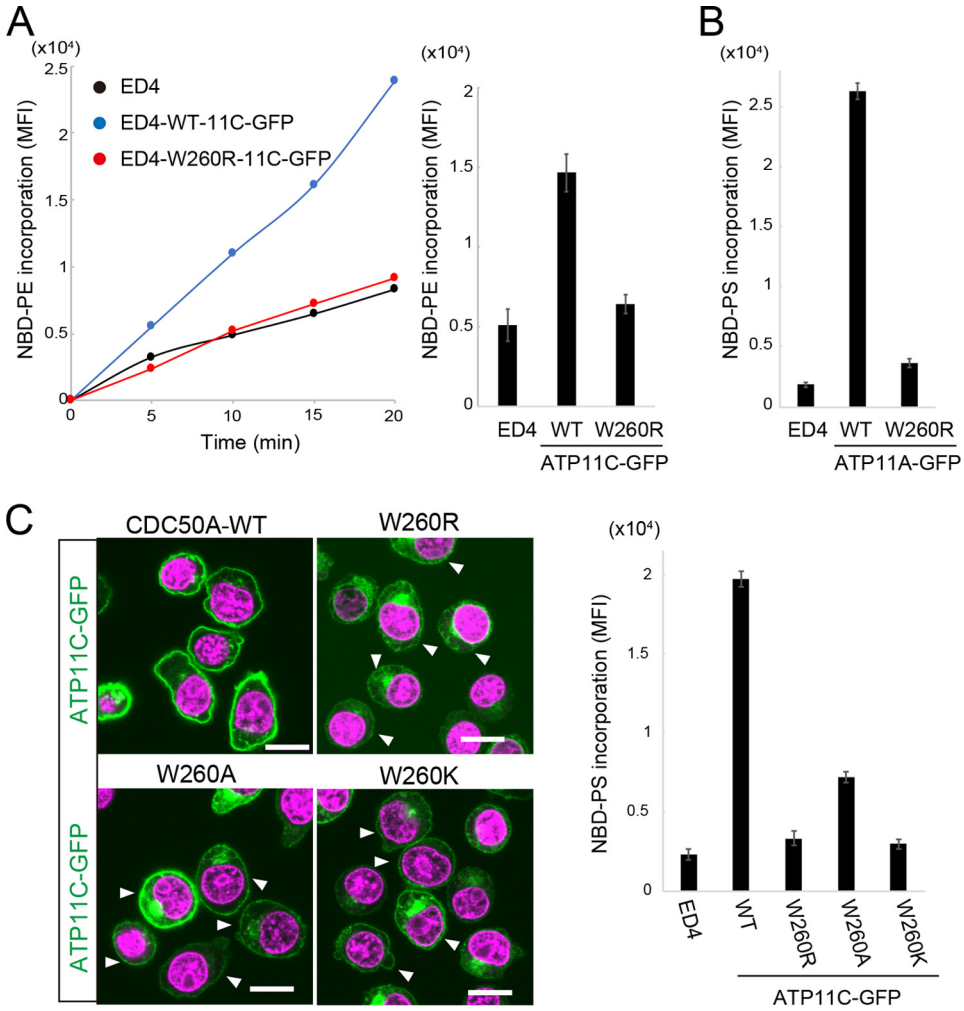


**Figure 6. Characterization of Trp-260 mutant.** *A*, ATP11C's flippase activity for PtdEtn. CDC50A$^{ED4}$ transformants expressing ATP11C with or without the wildtype or W260R mutant were incubated with NBD-PE for the indicated time (*left*) or 15 min (*right*), and the incorporated NBD-PE was determined using flow cytometry. *Right*, the mean MFI was plotted with S.D. ($n = 3$). *B*, ATP11A's flippase activity for PtdSer. CDC50A$^{ED4}$ transformants expressing ATP11A with or without the wildtype or W260R mutant were incubated with NBD-PS for 2 min, and the incorporated NBD-PS was determined using flow cytometry. The mean MFI was plotted with S.D. ($n = 3$). *C*, effect of different mutations in Trp-260. CDC50A$^{ED4}$ cells were co-transformed with GFP-conjugated hATP11C together with FLAG-tagged WT or the indicated mutant CDC50A and observed by confocal microscopy in the presence of 5 $\mu$M DRAQ5. GFP and DRAQ5 signals are shown in *green* and *magenta*, respectively. *Scale bar*, 10 $\mu$m. In the *right panel*, the flippase activity of the CDC50A$^{ED4}$ transformants expressing ATP11C with or without the wildtype or indicated mutants of hCDC50A was determined by the incorporation of NBD-PS using flow cytometry. The experiments were carried out three times, and the mean MFI was plotted with S.D. (*error bars*).

formation (29). To rule out the possibility that these residues were missed due to our mutagenesis strategy, the amino acid residues Leu-51, Arg-76, and Pro-300 of hCDC50A were mutated (Fig. 4). The expression of these mutants in *CDC50A*-null cells indicated that they had a full ability to support ATP11C's flippase activity.[3] The apparently different residues identified between yeast and human CDC50A may reflect the different assay systems. In any case, most of the residues identified in human CDC50A are well-conserved in yeast (Fig. 4), suggesting that these residues may also play an important role in yeast CDC50's chaperone activity. Although there is a well-conserved stretch in the N-terminal cytoplasmic region of hCDC50, no mutants were identified in this region, which may suggest that the N-terminal sequence does not contribute to the ability of the heterodimer to exit the ER. This observation agrees with the minimal contribution of the cytoplasmic region of the $\beta$-subunit of Na,K-ATPase, a member of the P2-ATPase family, for its chaperone activity (30, 31).

Our identified hCDC50A mutants could be categorized into two groups. In one group, to which most of the mutants belonged, the mutants could not function as a chaperone for P4-ATPases to their target locations. At least three of these mutants did not form a stable complex with ATP11C, and both ATP11C and the mutant CDC50A were localized to the ER (Fig. 5).[3] Together with the fact that P4-ATPase requires CDC50A as a chaperone to exit the ER, but its location is determined by the P4-ATPase (32), these results indicate that a motif or domain generated by the complex of P4-ATPase and CDC50A is recognized by the machinery that transports the complex from the ER to the target location. To transport molecules from the ER to the plasma membrane, an "ER-exit" machinery recognizes the "ER-exit signal" of the target molecule in the cytoplasm (33, 34). Elucidation of the tertiary structure of the P4-ATPase and CDC50A complex may reveal how

[3] K. Segawa and S. Nagata, unpublished results.

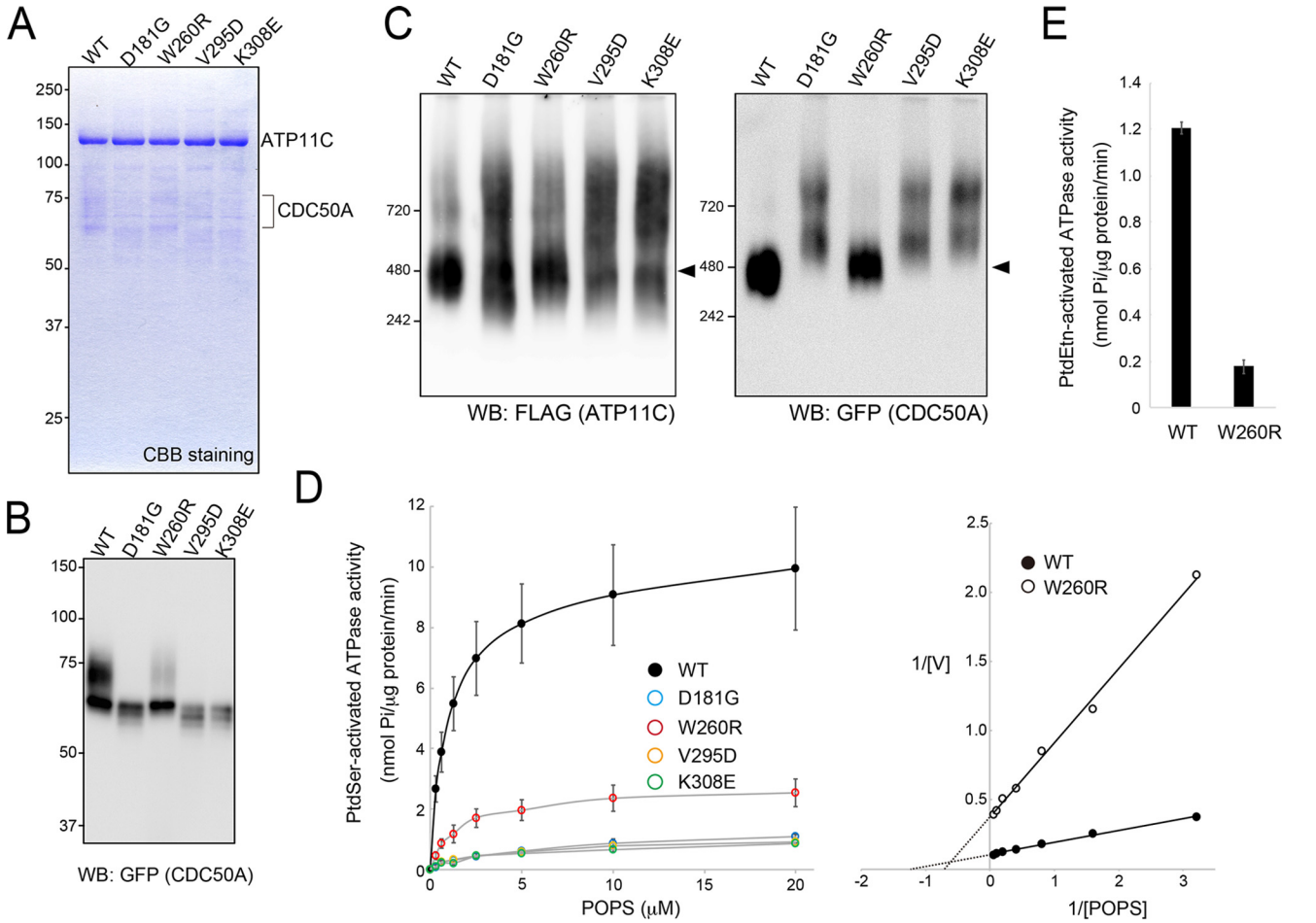


**Figure 7. Effect of CDC50A mutations on ATP11C's ATPase activity.** *A*, purification of the flippase complex of hATP11C and hCDC50A. FLAG-tagged hATP11C was expressed in 293T cells together with GFP-tagged WT or the indicated mutant hCDC50A and purified using anti-FLAG beads. The purified protein (150 ng) was separated by SDS-PAGE and stained with CBB. The FLAG-hATP11C and GFP-hCDC50A (about 60–75 kDa) are indicated. *B*, Western blotting for GFP-tagged CDC50A. The purified flippase complex (10 ng protein) was separated by SDS-PAGE and analyzed by Western blotting with an anti-GFP Ab. *C*, BN-PAGE analysis. The purified flippase (50 ng) was separated by BN-PAGE and analyzed by Western blotting with anti-FLAG for ATP11C or anti-GFP for CDC50A. *D* and *E*, ATPase activity of the purified flippase complex. The ATPase activity of the purified flippase complex (10 ng of protein) was determined in the presence of the indicated concentration of POPS (*D*) or 30 $\mu$M POPE (*E*). The PtdSer- or PtdEtn-activated ATPase activity (nmol of $P_i$/$\mu$g of protein/min) was determined by subtracting the ATPase activity without POPS or POPE. The experiments were performed three times, and the mean values are plotted with S.D. (*error bars*). The PtdSer-dependent ATPase activity of the ATP11C complexed with WT or W260R CDC50A was confirmed with another preparation of the purified enzymes. To the *right* of *D*, the mean values of the PtdSer-stimulated ATPase activity of ATP11C were plotted according to Lineweaver–Burk for PtdSer. The estimated maximal reaction rate ($V_{max}$) and PtdSer half-maximum activation constant ($K_a$) are as follows: WT, $V_{max}$ = 9.5 nmol of $P_i$/min/$\mu$g of protein, $K_a$ = 0.8 $\mu$M; W260R, $V_{max}$ = 2.7 nmol of $P_i$/min/$\mu$g of protein, $K_a$ = 1.4 $\mu$M. *WB*, Western blotting.

CDC50A's interaction with P4-ATPases exposes the ER-exit signal in the P4-ATPase.

The W260R mutant belonged to another group of CDC50A mutants, in which hATP11C and the CDC50A mutant formed a stable complex, yet the PtdSer- or PtdEtn-stimulated ATPase activity was severely reduced, suggesting that CDC50A is involved in the catalytic activity of the P4-ATPase. This finding was consistent with previous reports showing that CDC50 promotes the phosphorylation of a key aspartate residue in Drs2p, ATP8B1, and ATP8B2 (21, 35). Here again, how the extracellular region of CDC50 affects the ATPase activity of P4-ATPase, which carries the ATPase domain in its cytoplasmic region, is an interesting but challenging subject. Recently, Vestergaard *et al.* (36) reported that point mutations in transmembrane segments of ATP8A2 reduce the glycosylation or ER exit of CDC50A without affecting the ATPase activity of ATP8A2. Type II P-ATPases, such as $Ca^{2+}$ ATPase and Na,K ATPase, change their conformation during their catalytic cycle (37). It is possible that the structure of the P4-ATPase-CDC50 complex may differ between its ER-exit and its activated flippase states.

## Experimental procedures

### *Cell lines, plasmids, antibodies, and reagents*

W3 cells are mouse T-cell lymphoma (WR19L) cells that express mouse Fas (38). W3-Ildm cells are WR19L cells that express Fas and a caspase-resistant form of ICAD (inhibitor of caspase-activated DNase) (39). $CDC50A^{ED29}$ is a *CDC50A*-null W3-Ildm cell line that was established by CRISPR-Cas9–mediated gene editing (12). $CDC50A^{ED4}$, a *CDC50A*-null W3 line, was similarly established (Fig. S3). W3, W3Ildm, and their derivatives were cultured in RPMI 1640 supplemented with 10% FCS. HEK293T cells were cultured in DMEM containing 10% FCS.

pMXs-puro retroviral vector and pGag-pol-IRES-bsr packaging plasmid (40) were provided by T. Kitamura (Institute of

Medical Science, University of Tokyo). pCMV-VSV-G plasmid was from H. Miyoshi (Riken Bioresource Center). pAdVAntage was purchased from Thermo Fisher Scientific. Human cDNAs for *CDC50A* (NM_018247.3), *ATP10B* (NM_025153.2), and *ATP11A* (NM_015205.2, carrying SNP rs11616795 and rs368865), and *ATP11C* (XM_005262405.1) were described previously (11). These cDNAs were tagged with FLAG or GFP at the C terminus and inserted into pMXs-puro. pMXs-puro-GFP is the pMXs-puro vector used to express a C-terminally GFP-tagged molecule. The single-point mutants of hCDC50A were prepared by recombinant PCR (41) with complementary primers carrying mutated nucleotides (Table S3), and their sequence authenticity was verified by sequencing.

HRP-conjugated rabbit anti-GFP Ab was from Medical & Biological Laboratories. HRP-conjugated anti-FLAG M2 mAb and anti-FLAG M2–conjugated magnetic beads were from Sigma-Aldrich. DRAQ5, LysoTracker Red DND-99, and Sytox Blue were from Thermo Fisher Scientific. NBD-PS, 1-oleoyl-2-{6-[(7-nitro-2–1,3-benzoxadiazol-4-yl)amino] hexanoyl}-*sn*-glycero-3-phosphorethanolamine (NBD-PE), 1-palmitoyl-2-oleoyl-*sn*-glycero-3-phospho-L-serine (POPS), and 1-palmitoyl-2-oleoyl-*sn*-glycero-3-phosphoethanolamine (POPE) were from Avanti Polar Lipids.

### *Library of CDC50A mutants*

*hCDC50A* cDNA was mutagenized using the GeneMorph II Random Mutagenesis Kit (Agilent Technologies). The mutation frequency was adjusted to a few mutations per cDNA by changing the amount of template DNA and the PCR cycle number. In brief, mutations were introduced with 6 $\mu$g of plasmid DNA (pMXs-puro-hCDC50A) by performing 9 cycles of PCR with the following primers: 5′-GGCTTAATTAACCCAGGGATCGATG-3′ and 5′-GGCGAATTCAATGGTAATGTCAGCTG-3′ (PacI and EcoRI sites are underlined). The amplicons were digested with PacI and EcoRI, ligated with pMXs-puro-GFP, and introduced into *E. coli* (Endura$^{TM}$ competent cells, Lucigen) by electroporation using a Gene Pulser (Bio-Rad). Approximately $1 \times 10^7$ clones were obtained, and the plasmid DNA was prepared as the hCDC50A mutant library.

### *Screening for cells expressing mutant CDC50A*

HEK293T cells ($4 \times 10^6$) were transfected with 7.2 $\mu$g of hCDC50A mutant library plasmid DNA using FuGENE6 (Promega) together with 2 $\mu$g of pGag-pol-IRES-bsr, 1.4 $\mu$g of pCMV-VSV-G, and 1.4 $\mu$g of pAdVAantage$^{TM}$ and incubated for 48 h. Retroviruses in the supernatants were passed through a 0.45-$\mu$m polyvinylidene difluoride (PVDF) membrane (Merck Millipore), concentrated by centrifugation at 6000 $\times$ *g* for 16 h at 4 °C, and suspended in 500 $\mu$l of RPMI containing 10% FCS. The virus solution was diluted 625-fold with the culture medium containing 10 $\mu$g/ml Polybrene and used for the spin infection (700 $\times$ *g* for 1 h at 30 °C) of $3.8 \times 10^7$ CDC50A$^{ED29}$ cells that had been seeded at $5 \times 10^4$ cells/well in 24-well dishes (Corning). The infected cells were cultured for 3 days, and CDC50A$^{ED29}$ transformants expressing GFP (about $1.5 \times 10^7$ cells) were sorted by flow cytometry with a FACSAria II and expanded. The GFP-positive cells ($3 \times 10^7$) were then incubated for 5 min at 20 °C in 3 ml of Hanks' balanced salt solution (HBSS) containing 2 mM $CaCl_2$, 1 mM $MgCl_2$, and 1 $\mu$M NBD-PS, collected by centrifugation, mixed with prechilled HBSS containing 5 mg/ml fatty acid–free BSA to remove non-incorporated NBD-PS, and subjected to flow cytometry with the FACSAria II. The cells displaying low fluorescence were collected and expanded. This procedure consisting of incubation with NBD-PS and FACS sorting was repeated, and the resultant flippase-defective cells were designated as LF cells.

### *Deep sequencing and data processing*

Genomic DNA was purified from the LF cells using the QIAamp DNA minikit (Qiagen), and the integrated *hCDC50A* cDNA was amplified by PCR using PrimeSTAR GXL DNA polymerase (Takara) with primers (5′-GGCAGCCTACCAAGAACAAC-3′ and 5′-AAGTCGTGCTGCTTCATGTG-3′) located at about 200 bp downstream and upstream of the *hCDC50A* cDNA, respectively. To ensure high coverage, 25-cycle PCR in a 50-$\mu$l reaction volume was carried out with 280 ng of LF cell DNA 40 times, and 19-cycle PCR with 40 ng of plasmid DNA of the hCDC50A mutant library was performed 10 times. The PCRs yielded 11 and 0.4 $\mu$g of DNA for the LF cell genomic DNA and CDC50A mutant plasmid DNA library, respectively.

Each PCR product was pooled, purified with a spin column (Promega), quantified by the Quant-iT$^{TM}$ PicoGreen® dsDNA assay kit (Thermo Fisher Scientific), and subjected to deep sequencing. In brief, the PCR product (8 ng) was "tagmented" and amplified with the Nextra® XT DNA library preparation kit (Illumina) and subjected to massive DNA sequencing with the MiSeq platform (Illumina). The obtained reads were aligned with the reference hCDC50A sequence using the BWA-MEM algorithm (http://bio-bwa.sourceforge.net)[4] (42), and the number of alleles that agreed or did not agree with the reference was counted. The error frequency of non-reference alleles to the total alleles was calculated for each nucleotide and amino acid position. The read-processing procedure for determining error frequencies was designed as a custom order at Amelieff Co.

### *Characterization of CDC50A mutants*

To analyze the function of CDC50A mutants, retroviruses carrying each FLAG-tagged *CDC50A* mutant cDNA were produced using the pMXs-puro vector. CDC50A$^{ED4}$ cells were infected with retrovirus carrying the FLAG-tagged CDC50A mutants, and the transformants were selected with 1 $\mu$g/ml puromycin. These transformants were then infected with retrovirus carrying GFP-tagged P4-ATPases (ATP10B, ATP11A, or ATP11C), and the GFP-positive cells were isolated. The flippase activity of the transformants was then assayed as described above. In brief, $2 \times 10^5$ cells were incubated with 1 $\mu$M NBD-PS or NBD-PE at 15 °C in 150 $\mu$l of HBSS containing 1 mM $MgCl_2$ and 2 mM $CaCl_2$, collected by centrifugation, suspended in HBSS containing 5 mg/ml fatty acid–free BSA, and analyzed by a FACSCanto II. For microscopic analysis, $2–4 \times 10^5$ cells were suspended in HBSS containing 2% FCS and incubated at room temperature with 5 $\mu$M DRAQ5 for 3 min or at 37 °C with

[4] Please note that the JBC is not responsible for the long-term archiving and maintenance of this site or any other third party hosted site.

100 nM LysoTracker for 30 min, plated on a glass-bottom dish (Iwaki, AGC Techno Glass), and observed with a confocal microscope (FV1000-D; Olympus).

### *Purification of the flippase complex and ATPase assay*

Recombinant flippase was produced, purified, and subjected to the ATPase assay as described previously (11). In brief, $1.5 \times 10^8$ HEK293T cells were co-transfected using polyethyleneimine- mediated delivery (43) with 600 $\mu$g of pEF-BOS vector carrying *FLAG-hATP11C* and the same vector carrying *GFP-hCDC50A* or its mutants. The cells were lysed with solubilization buffer (40 mM MES/Tris buffer (pH 7.0), 5 mM $MgCl_2$, 150 mM NaCl, 10% glycerol, 0.5 mM DTT, 0.5% lauryl maltose-neopentyl glycol (LMNG), and a mixture of protease inhibitors (cOmplete, Mini, EDTA-free; Roche Diagnostics)). The cell lysates were applied to anti-FLAG M2-beads, and the bound proteins were eluted with 160 $\mu$g/ml 3×FLAG peptide (Sigma-Aldrich) in 40 mM MES/Tris buffer (pH 7.0) containing 150 mM NaCl, 10% glycerol, 0.5 mM DTT, and 0.05% LMNG (elution buffer). This procedure yielded a few $\mu$g of the purified flippase complex.

To assay the ATPase activity, the purified protein (~10 ng) was successively incubated for 10 min at room temperature and for 20 min at 37 °C in the reaction buffer (40 mM MES/Tris buffer (pH 7.0), 5 mM $MgCl_2$, 150 mM NaCl, 600 $\mu$M ATP, 5% glycerol, 5 mM DTT, and 0.05% LMNG). The released phosphate was reacted with malachite green oxalate and ammonium heptamolybdate tetrahydrate in the presence of polyvinylalcohol, and the resulting malachite green–molybdate phosphate complex was detected at 610 nm using a microplate reader (Infinite M200; Tecan).

### *SDS-PAGE, BN-PAGE, and Western blotting*

For SDS-PAGE, the purified flippase sample was incubated for 20 min at room temperature in SDS sample buffer (66 mM Tris-HCl buffer (pH 6.8), 2% SDS, 10% glycerol, 1% $\beta$-mercaptoethanol, and 0.003% bromphenol blue) and separated by electrophoresis on a 10% polyacrylamide gel (Nacalai). Precision Plus protein standards (Bio Rad) were used as molecular weight markers.

BN-PAGE was carried our essentially as described previously (44). Briefly, the purified flippase complex (50 ng of protein) in the elution buffer was mixed with 5% CBB G-250 to a final concentration of 0.5% and loaded onto NativePAGE™ Novex® 4–16% BisTris gels (Life Technologies, Inc.). After electrophoresis at 150 V for 35 min at 4 °C, the concentration of CBB G-250 in the running buffer was changed from 0.02 to 0.002%, and the samples were subjected to further electrophoresis at 150 V for 120 min. A protein standard (Thermo Fisher Scientific), consisting of IgM hexamer (1236 kDa), IgM pentamer (1048 kDa), apoferritin (720 and 480 kDa), B-phycoerythrin (242 kDa), lactate dehydrogenase (146 kDa), BSA (66 kDa), and soybean trypsin inhibitor (20 kDa), was used as molecular weight markers.

For Western blotting, proteins in gels were transferred to PVDF membranes immediately after SDS-PAGE or after incubating a BN-PAGE gel in SDS loading buffer (25 mM Tris-HCl (pH 8.3), 192 mM glycine, and 0.1% SDS). The membranes were probed with HRP-conjugated anti-FLAG M2 mAb or rabbit anti-GFP Ab, followed by detection with Immobilon Western Chemiluminescent HRP substrate (Merck Millipore). In some cases, the proteins were stained with CBB R-250.

*Author contributions*—K.S. and S.N. conceptualization; K.S. data curation; K.S. and S.N. funding acquisition; K.S. and S.N. validation; K.S. and S.K. investigation; K.S. writing-original draft; K.S. and S.N. writing-review and editing; S.N. project administration.

*Acknowledgments—We thank K. Yamada for technical assistance and M. Fujii for secretarial assistance.*

## References


1. Leventis, P. A., and Grinstein, S. (2010) The distribution and function of phosphatidylserine in cellular membranes. *Annu. Rev. Biophys.* **39,** 407–427 CrossRef Medline
2. van Meer, G., Voelker, D. R., and Feigenson, G. W. (2008) Membrane lipids: where they are and how they behave. *Nat. Rev. Mol. Cell Biol.* **9,** 112–124 CrossRef Medline
3. Bevers, E. M., and Williamson, P. L. (2016) Getting to the outer leaflet: physiology of phosphatidylserine exposure at the plasma membrane. *Physiol. Rev.* **96,** 605–645 CrossRef Medline
4. Fadok, V. A., de Cathelineau, A., Daleke, D. L., Henson, P. M., and Bratton, D. L. (2001) Loss of phospholipid asymmetry and surface exposure of phosphatidylserine is required for phagocytosis of apoptotic cells by macrophages and fibroblasts. *J. Biol. Chem.* **276,** 1071–1077 CrossRef Medline
5. Nagata, S., Hanayama, R., and Kawane, K. (2010) Autoimmunity and the clearance of dead cells. *Cell* **140,** 619–630 CrossRef Medline
6. Lhermusier, T., Chap, H., and Payrastre, B. (2011) Platelet membrane phospholipid asymmetry: from the characterization of a scramblase activity to the identification of an essential protein mutated in Scott syndrome. *J. Thromb. Haemost.* **9,** 1883–1891 CrossRef Medline
7. Kornberg, R. D., and McConnell, H. M. (1971) Inside-outside transitions of phospholipids in vesicle membranes. *Biochemistry* **10,** 1111–1120 CrossRef Medline
8. Andersen, J. P., Vestergaard, A. L., Mikkelsen, S. A., Mogensen, L. S., Chalat, M., and Molday, R. S. (2016) P4-ATPases as phospholipid flippases: structure, function, and enigmas. *Front. Physiol.* **7,** 275 Medline
9. Hankins, H. M., Baldridge, R. D., Xu, P., and Graham, T. R. (2015) Role of flippases, scramblases and transfer proteins in phosphatidylserine subcellular distribution. *Traffic* **16,** 35–47 Medline
10. Takatsu, H., Tanaka, G., Segawa, K., Suzuki, J., Nagata, S., Nakayama, K., and Shin, H. W. (2014) Phospholipid flippase activities and substrate specificities of human type IV P-type ATPases localized to the plasma membrane. *J. Biol. Chem.* **289,** 33543–33556 CrossRef Medline
11. Segawa, K., Kurata, S., and Nagata, S. (2016) Human type IV P-type ATPases that work as plasma membrane phospholipid flippases, and their regulation by caspase and calcium. *J. Biol. Chem.* **291,** 762–772 CrossRef Medline
12. Segawa, K., Kurata, S., Yanagihashi, Y., Brummelkamp, T. R., Matsuda, F., and Nagata, S. (2014) Caspase-mediated cleavage of phospholipid flippase for apoptotic phosphatidylserine exposure. *Science* **344,** 1164–1168 CrossRef Medline
13. Yabas, M., Jing, W., Shafik, S., Bröer, S., and Enders, A. (2016) ATP11C facilitates phospholipid translocation across the plasma membrane of all leukocytes. *PLoS One* **11,** e0146774–e0146712 CrossRef Medline
14. Yabas, M., Coupland, L. A., Cromer, D., Winterberg, M., Teoh, N. C., D'Rozario, J., Kirk, K., Bröer, S., Parish, C. R., Enders, A. (2014) Mice deficient in the putative phospholipid flippase ATP11C exhibit altered erythrocyte shape, anemia, and reduced erythrocyte life span. *J. Biol. Chem.* **289,** 19531–19537 CrossRef Medline
15. Arashiki, N., Takakuwa, Y., Mohandas, N., Hale, J., Yoshida, K., Ogura, H., Utsugisawa, T., Ohga, S., Miyano, S., Ogawa, S., Kojima, S., and Kanno, H.

(2016) ATP11C is a major flippase in human erythrocytes and its defect causes congenital hemolytic anemia. *Haematologica* **101,** 559–565 CrossRef Medline
16. Takatsu, H., Baba, K., Shima, T., Umino, H., Kato, U., Umeda, M., Nakayama, K., and Shin, H. W. (2011) ATP9B, a P4-ATPase (a putative aminophospholipid translocase), localizes to the *trans*-Golgi network in a CDC50 protein-independent manner. *J. Biol. Chem.* **286,** 38159–38167 CrossRef Medline
17. Coleman, J. A., and Molday, R. S. (2011) Critical role of the $\beta$-subunit CDC50A in the stable expression, assembly, subcellular localization, and lipid transport activity of the P4-ATPase ATP8A2. *J. Biol. Chem.* **286,** 17205–17216 CrossRef Medline
18. Stanley, P. (2011) Golgi glycosylation. *Cold Spring Harb. Perspect. Biol.* **3** Medline
19. Heuberger, E. H., Veenhoff, L. M., Duurkens, R. H., Friesen, R. H. E., and Poolman, B. (2002) Oligomeric state of membrane transport proteins analyzed with blue native electrophoresis and analytical ultracentrifugation. *J. Mol. Biol.* **317,** 591–600 CrossRef Medline
20. Zhang, L., Yang, Y., Li, S., Zhang, S., Zhu, X., Tai, Z., Yang, M., Liu, Y., Guo, X., Chen, B., Jiang, Z., Lu, F., and Zhu, X. (2017) Loss of Tmem30a leads to photoreceptor degeneration. *Sci. Rep.* **7,** 9296 CrossRef Medline
21. Lenoir, G., Williamson, P., Puts, C. F., and Holthuis, J. C. M. (2009) Cdc50p plays a vital role in the ATPase reaction cycle of the putative aminophospholipid transporter Drs2p. *J. Biol. Chem.* **284,** 17956–17967 CrossRef Medline
22. Takahashi, Y., Fujimura-Kamada, K., Kondo, S., and Tanaka, K. (2011) Isolation and characterization of novel mutations in CDC50, the noncatalytic subunit of the Drs2p phospholipid flippase. *J. Biochem.* **149,** 423–432 CrossRef Medline
23. Puts, C. F., Panatala, R., Hennrich, H., Tsareva, A., Williamson, P., and Holthuis, J. C. M. (2012) Mapping functional interactions in a heterodimeric phospholipid pump. *J. Biol. Chem.* **287,** 30529–30540 CrossRef Medline
24. García-Sánchez, S., Sánchez-Cañete, M. P., Gamarro, F., and Castanys, S. (2014) Functional role of evolutionarily highly conserved residues, *N*-glycosylation level and domains of the Leishmaniamiltefosine transporter-Cdc50 subunit. *Biochem. J.* **459,** 83–94 CrossRef Medline
25. Fowler, D. M., Stephany, J. J., and Fields, S. (2014) Measuring the activity of protein variants on a large scale using deep mutational scanning. *Nat. Protoc.* **9,** 2267–2284 CrossRef Medline
26. Robins, W. P., Faruque, S. M., and Mekalanos, J. J. (2013) Coupling mutagenesis and parallel deep sequencing to probe essential residues in a genome or gene. *Proc. Natl. Acad. Sci. U.S.A.* **110,** E848–E857 CrossRef Medline
27. Shin, H., and Cho, B.-K. (2015) Rational protein engineering guided by deep mutational scanning. *Int. J. Mol. Sci.* **16,** 23094–23110 CrossRef Medline
28. Labrou, N. E. (2010) Random mutagenesis methods for *in vitro* directed enzyme evolution. *Curr. Protein Pept. Sci.* **11,** 91–100 CrossRef Medline
29. Costa, S. R., Marek, M., Axelsen, K. B., Theorin, L., Pomorski, T. G., and López-Marqués, R. L. (2016) Role of post-translational modifications at the $\beta$-subunit ectodomain in complex association with a promiscuous plant P4-ATPase. *Biochem. J.* **473,** 1605–1615 CrossRef Medline
30. Hamrick, M., Renaud, K. J., and Fambrough, D. M. (1993) Assembly of the extracellular domain of the Na,K-ATPase $\beta$ subunit with the $\alpha$ subunit: analysis of $\beta$ subunit chimeras and carboxyl-terminal deletions. *J. Biol. Chem.* **268,** 24367–24373 Medline
31. Renaud, K. J., Inman, E. M., and Fambrough, D. M. (1991) Cytoplasmic and transmembrane domain deletions of Na,K-ATPase $\beta$-subunit: effects on subunit assembly and intracellular transport. *J. Biol. Chem.* **266,** 20491–20497 Medline
32. López-Marqués, R. L., Poulsen, L. R., Hanisch, S., Meffert, K., Buch-Pedersen, M. J., Jakobsen, M. K., Pomorski, T. G., and Palmgren, M. G. (2010) Intracellular targeting signals and lipid specificity determinants of the ALA/ALIS P4-ATPase complex reside in the catalytic ALA $\alpha$-subunit. *Mol. Biol. Cell* **21,** 791–801 CrossRef Medline
33. Borgese, N. (2016) Getting membrane proteins on and off the shuttle bus between the endoplasmic reticulum and the Golgi complex. *J. Cell Sci.* **129,** 1537–1545 CrossRef Medline
34. D'Arcangelo, J. G., Stahmer, K. R., and Miller, E. A. (2013) Vesicle-mediated export from the ER: COPII coat function and regulation. *Biochim. Biophys. Acta* **1833,** 2464–2472 CrossRef Medline
35. Bryde, S., Hennrich, H., Verhulst, P. M., Devaux, P. F., Lenoir, G., and Holthuis, J. C. M. (2010) CDC50 proteins are critical components of the human class-1 P4-ATPase transport machinery. *J. Biol. Chem.* **285,** 40562–40572 CrossRef Medline
36. Vestergaard, A. L., Mikkelsen, S. A., Coleman, J. A., Molday, R. S., Vilsen, B., and Andersen, J. P. (2015) Specific mutations in mammalian P4-ATPase ATP8A2 catalytic subunit entail differential glycosylation of the accessory CDC50A subunit. *FEBS Lett.* **589,** 3908–3914 CrossRef Medline
37. Toyoshima, C., and Cornelius, F. (2013) New crystal structures of PII-type ATPases: excitement continues. *Curr. Opin. Struct. Biol.* **23,** 507–514 CrossRef Medline
38. Ogasawara, J., Watanabe-Fukunaga, R., Adachi, M., Matsuzawa, A., Kasugai, T., Kitamura, Y., Itoh, N., Suda, T., and Nagata, S. (1993) Lethal effect of the anti-Fas antibody in mice. *Nature* **364,** 806–809 CrossRef Medline
39. Sakahira, H., Enari, M., and Nagata, S. (1998) Cleavage of CAD inhibitor in CAD activation and DNA degradation during apoptosis. *Nature* **391,** 96–99 CrossRef Medline
40. Kitamura, T., Koshino, Y., Shibata, F., Oki, T., Nakajima, H., Nosaka, T., and Kumagai, H. (2003) Retrovirus-mediated gene transfer and expression cloning: powerful tools in functional genomics. *Exp. Hematol.* **31,** 1007–1014 CrossRef Medline
41. Higuchi, R. (1990) Recombinant PCR. In *PCR Protocols: A Guide to Methods and Applications*, Academic Press, Inc., pp. 177–188, San Diego, CA
42. Li, H., and Durbin, R. (2010) Fast and accurate long-read alignment with Burrows–Wheeler transform. *Bioinformatics* **26,** 589–595 CrossRef Medline
43. Raymond, C., Tom, R., Perret, S., Moussouami, P., L'Abbé, D., St-Laurent, G., and Durocher, Y. (2011) A simplified polyethylenimine-mediated transfection process for large-scale and high-throughput applications. *Methods* **55,** 44–51 CrossRef Medline
44. Suzuki, J., Imanishi, E., and Nagata, S. (2016) Xkr8 phospholipid scrambling complex in apoptotic phosphatidylserine exposure. *Proc. Natl. Acad. Sci. U.S.A.* **113,** 9509–9514 CrossRef Medline
45. Katoh, K., Rozewicki, J., and Yamada, K. D. (2017) MAFFT online service: multiple sequence alignment, interactive sequence choice and visualization. *Brief. Bioinform.* 10.1093/bib/bbx108 CrossRef Medline